

See discussions, stats, and author profiles for this publication at: <https://www.researchgate.net/publication/231289809>

Floc Architecture in Wastewater and Natural Riverine Systems

ARTICLE *in* ENVIRONMENTAL SCIENCE AND TECHNOLOGY · JANUARY 1996

Impact Factor: 5.33 · DOI: 10.1021/es950426r

CITATIONS

129

READS

58

4 AUTHORS, INCLUDING:



Ian G. Droppo

Environment Canada

124 PUBLICATIONS 2,618 CITATIONS

SEE PROFILE



Gary Leppard

Environment Canada

95 PUBLICATIONS 3,923 CITATIONS

SEE PROFILE

Floc Architecture in Wastewater and Natural Riverine Systems

STEVEN N. LISS,^{*,†} IAN G. DROPPA,[‡]
DERRICK T. FLANNIGAN,[§] AND
GARY G. LEPPARD^{‡,§}

*Department of Applied Chemical & Biological
Sciences, Ryerson Polytechnic University,
Toronto, Ontario M5B 2K3, Canada, National
Water Research Institute, Environment Canada,
Burlington, Ontario L7R 4A6, Canada, and
Department of Biology, McMaster University,
Hamilton, Ontario L8S 4K1, Canada*

The study of flocs has largely been devoted to the gross ($>1\ \mu\text{m}$) scale so that the behavior of flocs (i.e., transport and settling) can be observed and modeled. With the assistance of a newly developed field kit and correlative microscopy [which includes transmission electron microscopy (TEM), scanning confocal laser microscopy (SCLM), and conventional optical microscopy (COM)], this paper begins to bridge the resolution gap between the gross and fine (sub-micron) scales in order to better understand the role of floc ultrastructure in outward floc behavior for both natural and engineered systems. Results from both systems have demonstrated that pores which appeared to be devoid of physical structures under the optical microscopic techniques (SCLM and COM) were observed to be composed of complex matrices of polymeric fibrils (4–6 nm diameter) when viewed by high-resolution TEM. These fibrils were found to represent the dominant physical bridging mechanism between organic and inorganic components of the flocs and contributed to the extensive surface area per unit volume of the flocs. In this way, the microbial floc resembles a biofilm and will likely support similar processes with respect to contaminants and the physical–chemical environment.

Introduction

Flocculated particles are central to a number of significant environmental processes within engineered and natural systems. They can be defined as sedimenting units which can be isolated by cascade filtration and ultracentrifugation (1–3) and are composed of two or more primary particles (e.g., a bacterial cell and an inorganic particle) (4). Microbial flocs have typically been seen as structural entities serving only to transport/settle sediment and contaminants in

natural or wastewater treatment systems. This approach has been restricted to the gross scale ($>1\ \mu\text{m}$) and has focused primarily on size, shape, density, porosity, and settling velocity for the purpose of modeling and manipulating sediment and contaminant fate and effect. At the fine scale (submicron), the importance of the microorganisms and bioorganic material to floc development and properties is well recognized (5). Visual observations of natural flocs with high-resolution electron–optical microscopy techniques have revealed cross-linkages of floc primary particles by bridges of fibrillar extracellular polymeric substances (fibrils), 2–10 nm in diameter (6). Fibrils can be detected in pelagic associations between microbes and abiotic particles (7) and are common components of freshwater ecosystems (4, 7–9). These fibrillar extracellular polymeric substances are an important class of microbially-derived colloids (particles $<1\ \mu\text{m}$ in the least dimension) as they may have a potential impact on the chemical, physicochemical, and biological processes within the floc itself and in the natural and engineered aquatic environment as a whole (3, 10, 11). The significance of this material to the internal floc ecosystem and outward gross floc behavior is, however, not fully understood.

This paper describes a multimicroscopic method for studying natural riverine and engineered flocs which reveals the internal architecture of flocculated particles. In doing so, a more realistic understanding of the internal microenvironment and outward behavior of biological flocs can be achieved. This will improve our knowledge of natural sediment dynamics and associated contaminant source, fate, and effect, as well as have significant implications for the manipulation of the internal fine-floc matrix for the management of engineered systems.

Experimental Section

Description of Sample Sites. Natural floc material was collected from the Nith River above Nithburg, Ontario, 20 July 1993. The river basin is predominantly agricultural in land use and primarily transports fine grained sediment (silts and clays) in suspension. The suspended solids concentration at the time of sampling was approximately $20\ \text{mg}\cdot\text{L}^{-1}$ with an instantaneous discharge of $1.2\ \text{m}^3\cdot\text{s}^{-1}$. The cobble river bed was covered with a surficial fine-grained sediment laminae (12, 13) and isolated macrophyte beds in slower flowing sections of the river.

Engineered flocs were sampled from a pulp and paper mill oxygenated activated sludge effluent system (OASES) serving Avenor, Inc., Thunder Bay, Ontario. Combined wastewater from the acid, alkaline, and neutral sewers of the bleached kraft pulp plant is pumped to a primary clarifier and then flows to the secondary treatment system at a rate of $80\ 000\ \text{m}^3\cdot\text{day}^{-1}$. On a daily basis, the treatment system typically received 39 tons per day (td) biochemical oxygen demand (BOD), 7 td suspended solids (SS), and 4.5 td total organo halogens (TOX) (3.2 kg of adsorbable organo halides (AOX) per ton of kraft pulp). The OASES system consisted of two oxygen trains, each with a capacity of 14.4 ML. The hydraulic retention time was about 12 h. The system consumes 40 tons of oxygen per day (provided during aeration). After secondary treatment, on average, BOD discharges were $<4\ \text{tons}\cdot\text{day}^{-1}$ ($>50\ \text{mg}\cdot\text{L}^{-1}$), SS were $6\ \text{tons}\cdot\text{day}^{-1}$, and AOX levels were $2.5\ \text{tons}\cdot\text{day}^{-1}$.

* Author to whom all correspondence should be addressed; fax: (416) 979-5044; e-mail address: sliss@acs.ryerson.ca.

[†] Ryerson Polytechnic University.

[‡] National Water Research Institute.

[§] McMaster University.

Conventional Optical Microscopy: Sample Collection, Preparation, and Documentation. River-suspended sediment samples for gross sediment analysis were collected in 2, 5, and 10 mL chambers held parallel to the direction of flow. The chambers were capped under water and inverted to an upright position where the sediment was allowed to settle for 24 h onto an inverted microscope settling slide. Photographs at 100 \times magnification (10 \times objective) were taken for later analysis (14) using a Zeiss Axiovert 100 inverted microscope. As sediment concentrations were relatively low, an additional sample was collected in a 2 mL chamber by disturbing recently deposited fine-grain sediment laminae on the cobble river bed and sampling the resulting sediment plume. The resuspended sample plume had a concentration of approximately 286 mg \cdot L $^{-1}$. These samples examined on a gross scale by COM were also examined at a fine scale in a parallel study, using aliquots prepared for TEM.

Scanning Confocal Laser Microscopy: Sample Collection, Preparation, and Documentation. A subsample of an activated sludge grab sample was placed above a sterile 0.22 μ m Nuclepore filter held in a filter apparatus. The floc material was stained in a solution of fluorescein isothiocyanate (FITC) (2 mg \cdot mL $^{-1}$ of 10 mM Tris-HCl (pH 10.0)). The stained floc was washed three times with 0.1 M phosphate buffer (pH 7.0). The floc was allowed to settle onto the filter by gravity, and the stain and wash solutions were removed by pipette and by passage through the filter. The filter, containing the stained floc, was removed from the filter apparatus and placed onto a clean microscope slide. Seventy percent glycerol, in phosphate buffer containing *p*-phenylenediamine, was placed onto the filter which was then covered with a glass cover slip supported by cover slip glass shards (pillars) at the corners. The edges of the cover slip were sealed with nail polish.

Images of the stained floc were obtained by SCLM using a Zeiss Micro Systems LSM (Model LSM 10 BioMed). The SCLM was equipped with an argon laser with emission lines at 418 and 514 nm. An oil immersion lens (63 \times , 1.4 numerical aperture) was used with an electronic zoom of 30 \times . Image slices were collected at 1 μ m vertical intervals.

TEM: Sample Collection, Preparation, and Documentation. To stabilize and prepare samples on-site for subsequent processing, leading to the production of ultrathin sections for observation by TEM, we selected four different treatments to be applied to aliquots of each sample (Figure 1, a 4-fold multipreparatory method). These four treatments were used correlatively to overcome specific artifacts inherent to each one when used independently. For examinations of the floc matrix, the principal artifacts of concern were excessive extraction and shrinkage; problems of low contrast also had to be addressed.

Using a newly developed field kit containing premeasured volumes of fixatives (Figure 1) and appropriate utensils, the samples were fixed on site and returned to the laboratory on ice for additional preparation. Figure 1 outlines the multimethod approach to preparing samples for TEM. For the two methods involving aldehyde fixation, mixed liquor or river water grab samples were collected and aliquots immediately distributed into two 14.0 mL screw cap vials. The first vial contained 3% glutaraldehyde buffered with 0.1 M Na-cacodylate (pH 7.1), and the second vial contained the buffered glutaraldehyde, as above, with the addition of 0.1% ruthenium red (RR) (15, 16). An equal volume of sample was added to these vials, bringing the

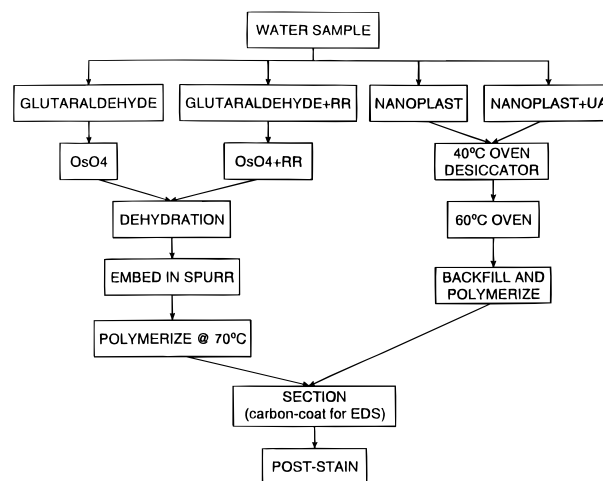


FIGURE 1. Four-fold multimethod preparatory technique for ultrastructural analysis of flocs.

final concentration of glutaraldehyde and RR to 1.5 and 0.05%, respectively (8, 17). The samples were held in a refrigerator overnight followed by centrifugation at 300g for 10 min and then washed three times in 0.1 M Na-cacodylate buffer (pH 7.1). The samples were finally resuspended in 1% osmium tetroxide (vial 1) or 1% osmium tetroxide plus 0.05% RR (vial 2). The samples were further incubated on ice for 1 h and then centrifuged and washed twice in buffer. The samples were then dehydrated (18) by means of an ethanol series for 5 min at each concentration: 30%, 50%, 70%, 90%, 95%, 100%, and 100%. At 70% the sample was allowed to reach room temperature. The samples were then placed in increasing concentrations of Spurr resin (19) and placed into molds. The resin was polymerized at 70 $^{\circ}$ C for 8 h. The procedure beginning with glutaraldehyde plus RR prevented the extraction of fibrils but produced a coarse image of details at high magnification. Both procedures suffered from uncontrolled matrix shrinkage brought about by the solvent dehydration step, although the shrinkage was not severe. The shrinkage is prevented by the Nanoplast procedures described below.

The remaining two vials (Figure 1) each contained a micromold capsule with ca. 200 μ L of Nanoplast resin (20, 21), a hydrophilic melamine embedding resin. In addition to Nanoplast, the fourth vial also contained 0.25% (w/w) uranyl acetate. One drop of sample from the end of a Pasteur pipet (ca. 50 μ L) was added to each and gently mixed with the end of a sterile wood toothpick. Upon return to the laboratory, the samples were put into a desiccator which was then placed in an oven at 40 $^{\circ}$ C. After 48 h, the capsules were removed from the desiccator and heated for a further 48 h, at 60 $^{\circ}$ C. The tubes containing the samples were then backfilled with Spurr resin and polymerized at 70 $^{\circ}$ C for 8 h. Nanoplast omits the solvent dehydration stage, and it forms cross-linkages between matrix colloids prior to structural water loss at the end of the embedding process. For this reason, measurements of the dimensions of colloidal matrix materials and their three-dimensional disposition are realistic (20). The addition of uranyl acetate as an enbloc stain corrects the low contrast problem for some matrix structures when using Nanoplast (22).

After polymerization, all samples were sectioned identically. Ultrathin sections for morphological studies (ca. 70 nm) and energy dispersive spectroscopy (EDS) analysis (ca. 100 nm) were obtained from the polymerized resins by

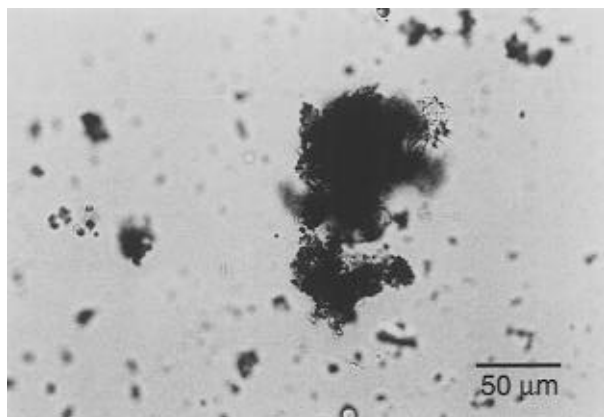


FIGURE 2. Unstained natural floc observed by conventional optical light microscopy (10X objective) (Nith River, Nithburg, Ontario, Canada).

sectioning with a diamond knife mounted in an ultramicrotome (RMC Ultramicrotome MT-7). The sections were mounted on formvar-covered copper grids. The grids used for EDS were carbon-coated for stabilization. The Spurr sections were counterstained with uranyl acetate and then lead citrate (6). The Nanoplast sections were counterstained with 1% aqueous uranyl acetate for 3–4 h.

The ultrathin sections were then observed in transmission mode (TEM) at an accelerating voltage of 80 kV using a JEOL 1200 EX II TEMSCAN scanning transmission electron microscope (STEM). The scanning mode of the STEM was used to generate a microprobe beam for EDS of individual floc components in sections. A Princeton Gamma Tech (PGT) Si[Li] X-ray detector and Imix multichannel analyzer provided spectra of all elements, with an atomic number greater than 10, on a “per colloid” basis.

Results and Discussion

Flocculated particles in both the natural and engineered environment are physically unstable, dynamic structures consisting of a microbial community and bioorganic (cellular debris and extracellular polymers) and inorganic material (4). The outward gross behavior of a floc (i.e., transport and settling) is generally the primary area of focus for wastewater management and for the prediction of contaminant fate in the natural aquatic system. This outward behavior is closely related to the internal fine structure of the flocculated particles. Currently, however, the role of the internal floc ultrastructure and activity on gross behavior is unclear. In order to investigate this fine structure it is necessary to use high-resolution microscopy (TEM) to increase the resolution over the optical microscopic techniques typically used for gross scale measurements (COM and SCLM) (23, 24).

Gross Structural Scale. When gross-scale visual observations of flocculated material are required, COM has generally been the technique of choice (14, 25, 26). Typical total magnification used is generally around 100× (10× objective) and will yield a lower resolution of approximately 1–2 μm when interfaced with image analysis software (12, 14). Figure 2 demonstrates a COM observation of fine-grained sediment obtained from the Nith River. Such imagery shows the entire floc structure and allows for an estimation of size, shape, volume, and particulate size distributions of the sediment in suspension (14). Descriptive observations of gross floc composition, density, and porosity can also be described with COM. Extreme caution

must be taken, however, when using COM for structural analysis as its limited resolution may provide erroneous observations as to the true structure of the floc matrix. This is particularly true for dense and/or large flocs which cannot be optically penetrated by COM and for the examination of floc pores and channels which may appear devoid of structure with COM but may in fact be a complex microcosm of polymers and biological activity when visualized at higher magnifications.

Some of the problems associated with COM can be resolved with SCLM through molecular probes and multiple optical sectioning. With SCLM and selected probes, individual bacteria can be differentiated and quantified and their spatial distribution within the floc derived through three-dimensional reconstruction of multiple optical slices (24, 27). Figure 3 demonstrates such an analysis for an activated sludge floc. Figure 3a–c illustrates selected optical sections and demonstrates the effectiveness by which digitization can provide quantitative information on the disposition of particles (bacteria) within a floc. Figure 3d shows the image of the total floc volume, as derived from a computerized stacking of optical sections obtained at 1 μm intervals. A complete chain of bacteria (see arrow) can be seen in Figure 3d, whereas only parts of this chain are visible in the individual sections. Through the use of selected molecular probes, SCLM may also differentiate bacterial species, viable versus nonviable bacteria, and diffusional gradients within the floc such as pH and redox potential (27).

Fine Structure Analysis. While SCLM has imaging advantages over COM (28), its resolving power is not sufficient for ultrastructural observations of individual fibrils within flocculated material. Such analysis can only be obtained by high-resolution (1 nm) TEM.

In order to view the internal structure of flocs at very high resolution, ultrathin sectioning is required. Such sectioning removes the sample thickness constraint on TEM imaging (6) but considerably restricts the sample volume which can be examined per unit of time. For very large flocs, the examination of 70 nm sections in sequence can be very costly and impractical if one wishes to examine the entire floc. In this regard, COM and SCLM images can be very useful as an indication of the number of TEM sections required for a collection of representative images of a floc. For example, the greater the heterogeneity of the floc observed by COM and SCLM, the greater the number of ultrathin sections required for TEM. If a floc appears to be very homogeneous, then considerably fewer sections will be required for a representative analysis. While TEM can bridge the resolution gap from the gross structure of sediment and the submicron ultrastructure, its usefulness is limited if not used in conjunction with the 4-fold multipreparatory method described in this paper. Multimethod preparation allows a systematic means of detection, assessment, and minimization of artifacts for the extraction of multilevel information.

The use of high resolution allows for detailed observations of the internal structure and composition of flocs otherwise not seen with COM and SCLM techniques. Figure 4a (fixed initially in glutaraldehyde) illustrates the presence of bacteria and inorganic clay particles within a natural riverine floc. This apparent relationship is likely related to the mineral particles representing a significant nutrient ion source and colonization site for autochthonous bacteria. Clay particles have a high affinity for the adsorption of

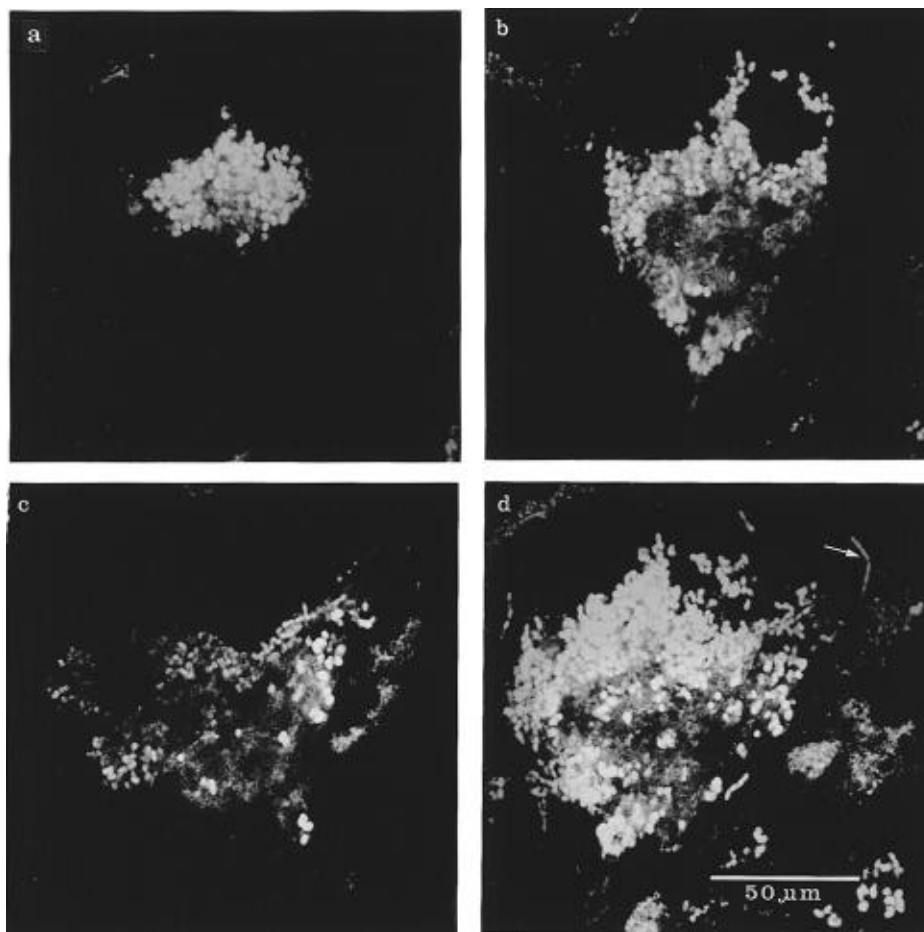


FIGURE 3. Biological floc material from activated sludge visualized by SCLM. Parts a–c represent optical sections from the floc taken at 8, 15, and 27 μm , respectively, from the bottom of the floc. Part d is a composite image derived from 29 serial sections taken at 1 μm vertical distance intervals.

nutrients and contaminants onto their surfaces (29). The bacteria–particle associations observed in Figure 4a, however, show no apparent attachment mechanism/structure for bacteria to other particles. Figure 4b,c, on the other hand, illustrate a possible mechanism with the aid of improved resolution (detail) through higher magnification and an additional preparation (Nanoplast counterstained with uranyl acetate). Figure 4b (fixed in glutaraldehyde) illustrates a section through a cell surrounded by a small amount of exopolymeric material. Although the exopolymeric material is sparse in this figure (due to its partial removal by extraction artifacts), microscopic observations of multiple serial sections revealed the existence of a three-dimensional network of such polymer material (fibrils). As less extraction resulted with the Nanoplast preparations, Figure 4c illustrates the more realistic dense network of exopolymeric material between the constituent organic and inorganic components of the floc. It is evident that the fibrils of exopolymeric material are an important structural component of the floc matrix as they are often a dominant entity within the large voids of the flocs as well as being associated with the surfaces of many of the inorganic clay particles and bacteria (Figure 4b,c). These extracellular polymers serve as a means of attachment and nutrient assimilation for many cells (30). This material also serves to stabilize the floc matrix and is likely the structural entity which promotes the pseudoplastic nature of flocculated material (14). Aggregation within this highly inorganic environment may also be influenced by electrochemical flocculation as is seen by the apparent inorganic

particle-to-particle contacts. EDS showed that the inorganic material consisted of Fe, Al/Si, and Si. Considering the spectra with the accompanying morphological information, the main inorganic particles were probably iron oxyhydroxides, clay minerals, and silicates, respectively (6).

Electron micrographs of ultrathin sections of typical flocs sampled from a bleached kraft pulp mill effluent treatment system are shown in Figure 5. Figure 5, parts a (glutaraldehyde plus RR) and b (glutaraldehyde fixed and counterstained) illustrate that bacteria are the dominant microbial component in the OASES. Greater than 90% of the bacteria were found to possess a typical Gram-negative cell wall. This is consistent with previous studies which revealed that Gram-negative bacteria represent the majority of culturable bacteria recovered from pulp mill effluent treatment systems (31, 32). While Figure 5b largely shows a floc composed of bacteria where there are large numbers of bacteria–bacteria associations, Figure 5a illustrates that many of the bacteria possess extracellular polymeric substances. Embedding flocs immediately upon sampling in water-miscible Nanoplast results in the preservation of the extracellular polymeric matrix which surrounds the bacterial cells and which appears to hold the floc structure together (Figure 5c,d). The proliferation of extracellular polymeric material (fibrils) observed in Figure 5c,d would suggest that the void space between cells observed in Figure 5a,b is completely filled with fibrillar material. Figure 5d shows the polymeric matrix at a higher magnification and illustrates that varying porosity and a high surface area per

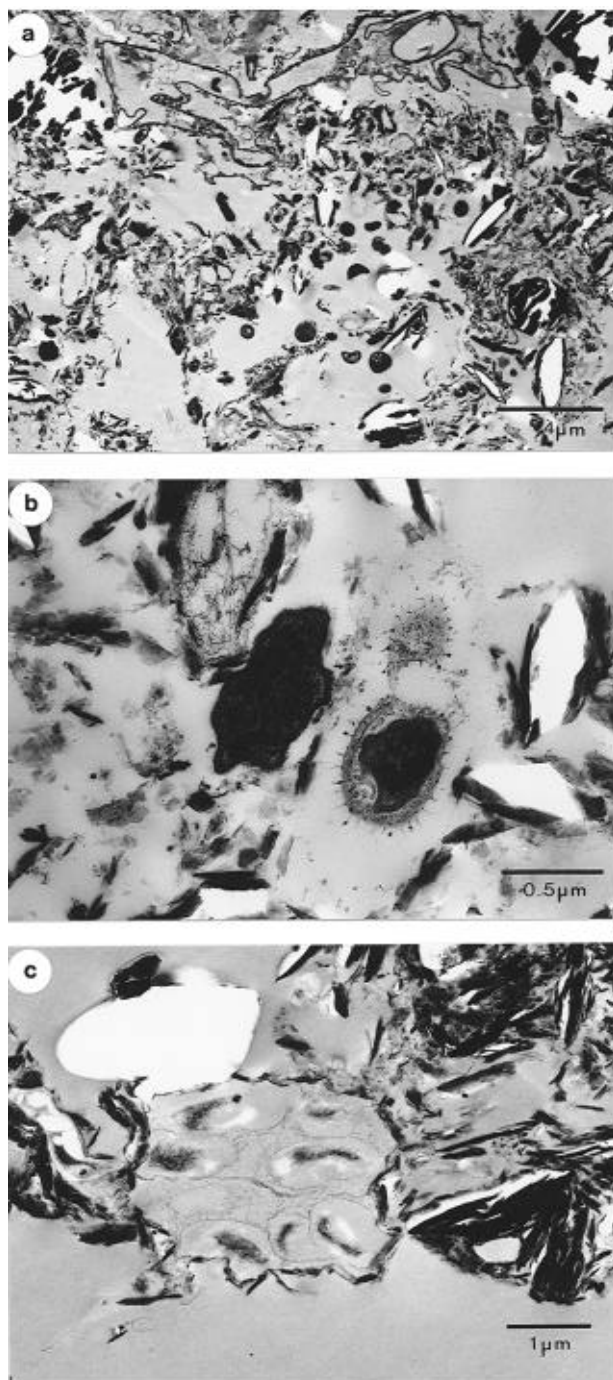


FIGURE 4. Electron micrographs of natural flocs sampled from the Nith River, Nithburg, Ontario, Canada: (a, b) sample was glutaraldehyde-fixed and counterstained; (c) sample was preserved in Nanoplast and counterstained with uranyl acetate (see Figure 1).

unit volume are characteristic of the floc structure. Individual fibrils on average had diameters in the 4–6 nm range. The fibrillar architecture visualized in Figures 4c and 5c,d is likely to approximate the native state because (a) no extracting fluids or washes were used in the TEM preparation; (b) the last stage of bound water loss occurred after the fibrils were fixed in position by Nanoplast polymer (minimal dehydration artifact); (c) no turbulence (i.e., no centrifugation and minimal sample handling) was imposed on the sample as it was fixed in place at the time of sampling; (d) there is no storage; and (e) aggregation/disaggregation problems (33) are minimized.

The floc shown in Figure 5c is a heterogeneous structure consisting of cells, bioorganic matrix, and electron dense inorganic material. EDS revealed that the inorganic material of this floc was similar to that found in the natural system (Fe, Al/Si, and Si).

This kind of image of minimally-perturbed fibril systems (the Nanoplast image) may have significant implications for the derivation of the true porosity of a floc. Traditional calculations of floc porosity have been indirectly dependent on the gross scale estimate of particle size, density, and settling velocity (25). Correlative microscopy, which includes high-resolution TEM, although only qualitative as described here, allows for the direct observation of ultra-structure (and to a limited extent, composition), with respect to the cellular, bioorganic, and inorganic components of the porous floc matrix. At this fine scale, it is evident that large pores are not necessarily open channels devoid of structural material, but rather encompass a complex matrix of polymeric fibrils. The polymeric matrix may promote resistance within the floc, potentially resulting in diffusional and electrochemical gradients. Gradients typically observed in sessile biofilms such as pH, O₂, redox, and substrate concentration (30) may be present within the floc and may support sequential (aerobic/anaerobic) processes (34). Calculations of pore water movement which do not take into consideration the internal structure of the pores may overestimate the flux of water in and out of the floc. The apparent fractal nature of the pore network suggests that flocs likely retain a greater quantity of water due to a large surface area and surface water tension. The ability of a floc to trap or replace pore water will also have a significant impact on the overall ecology, density, and settling characteristics of the floc.

Comparative Analysis. Characterization of the flocs from the engineered and natural systems reveals similar associations of structural entities, particularly with respect to the exopolymeric fibrils. Both floc types when viewed at high resolution (1 nm) resembled microbial biofilms described in the literature (30, 35, 36). We make the analogy that flocs may be envisioned as biofilms turned back on themselves so that the biofilm/substratum interface is internalized as the core of a suspended floc.

The natural flocs, as expected, contained a greater quantity of inorganic material than did the engineered flocs, whereas the flocs obtained from the wastewater treatment system were richer in cellular biomass. Fibrils acting as polymer bridges were frequently found as numerically-important components for both types of flocs. General similarities observed were sufficient to indicate that technology transfer from the analysis of one kind of floc to another would be effective. The detailed characterization of specific matrix colloids and their associations is required for the next stage of comparative analysis.

While the particle/colloid composition of both flocs is relatively similar, it is unlikely that the biological speciation and the physicochemical and ecophysiological relationships are the same. A multitude of factors (e.g., nutrient regime, oxygen, and pH) can affect both the population dynamics and floc structure in wastewater treatment and natural systems (4, 37, 38). The macromolecular components of the bacterial surface, which contribute to the floc structure (polysaccharide-rich exopolymers, lipopolysaccharides, and protein), have been shown to vary in quantity and composition with changes in growth conditions (30, 39). Changes in the chemical composition and properties of

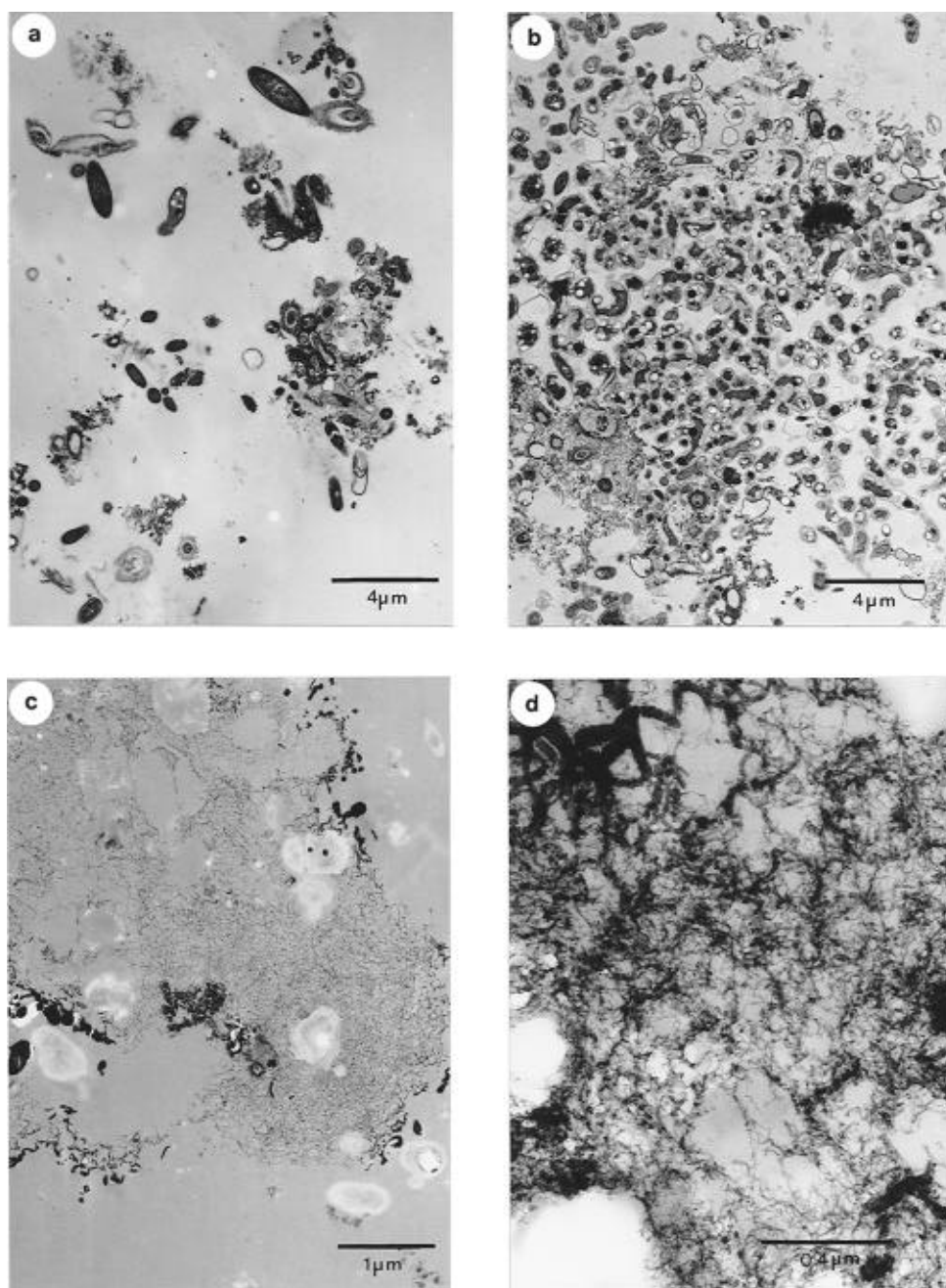


FIGURE 5. Electron micrographs of engineered flocs sampled from a bleached kraft pulp mill oxygenated activated sludge system: (a) sample was fixed initially in glutaraldehyde-ruthenium red fixative; (b) sample was glutaraldehyde-fixed and counterstained; (c, d) samples were preserved in Nanoplast (see Figure 1).

exopolymers in the floc matrix may also occur due to the sorption and concentration of contaminants on the surface of these materials (3, 11). A specific focus on the distribution of fibril types, as defined by selective staining (33), will help to visualize these changes. The chemical and physiological characteristics of the floc cannot necessarily be ascertained by structural analysis alone, but details of structure are likely to guide one in analyses of structure/chemistry/activity correlations relevant to floc roles in aquatic ecosystems.

Conclusion

A detailed study using correlative microscopy (COM, SCLM, and TEM) and a novel 4-fold multimethod preparatory technique for preserving samples immediately after sampling in the field has provided important structural

observations of the floc matrix from the gross to the fine scale. As demonstrated here, the use of multiple microscopes with overlapping resolution limits can provide unique insight into the structure of a floc. For example, COM provides valuable information on the gross morphological characteristics of a floc such as size and shape. This level of information can be useful for modeling sediment transport and settling. Using molecular probes, SCLM provides the added advantage of visualizing the three-dimensional disposition of various particles and potential diffusional gradients within the floc. Because of its 1 nm resolution, TEM, used in conjunction with the multimethod preparatory technique, provides fine details of the ultrastructural relationships within the network of the floc.

A comparative morphological study of engineered and natural flocs revealed similar cellular, bioorganic and

inorganic constituent particles, although they were present in different proportions. Common to both types of flocs was the significance of the fine polymeric extracellular fibrils which served to bind or bridge the particles together, providing structural support of an apparent pseudoplastic nature. Electrochemical flocculation was also observed but appeared to be a secondary floc building process compared to the extensive networks of polymeric fibrils. Large pores which appeared to be devoid of structure when observed with COM were often found to contain dense matrices of polymeric fibrils. These dense fibril networks will significantly increase the surface area available for the sorption of nutrients and contaminants and may promote resistance within the floc. This resistance may influence the floc's ability to trap or replace pore water as well as potentially resulting in diffusional and electrochemical gradients similar to those observed for biofilms with respect to contaminants, nutrients, oxygen, hydrogen ions, and oxidation–reduction potential. By viewing the structural detail of the floc matrix as a biofilm with regard to these processes, we may be able to better understand the outward behavior of flocs (i.e., transport and settling) and, potentially, learn how to better manipulate the physical, chemical, and/or biological characteristics of flocs for the benefit of an engineered system.

Acknowledgments

The authors wish to thank Ryerson Polytechnic University for a Seed Grant. The electron microscopy unit located in the Department of Biology, McMaster University, is supported by infrastructure funding provided by McMaster University and the Natural Sciences and Engineering Research Council (NSERC) of Canada. The research is funded by a NSERC Strategic Grant, STR0167324, awarded to S.N.L., I.G.D., and G.G.L.

Literature Cited

- (1) Filella, M.; Buffle, J.; Leppard, G. G. *Water Sci. Technol.* **1993**, *27*, 91–102.
- (2) Perret, D.; Newman, M. E.; Negre, J.-C.; Chen, Y.; Buffle, J. *Water Res.* **1994**, *28*, 91–106.
- (3) Leppard, G. G. In *Particulate Matter and Aquatic Contaminants*; Rao, S. S., Ed.; Lewis Publishers: Boca Raton, 1993; pp 169–195.
- (4) Droppo, I. G.; Ongley, E. D. *Water Res.* **1994**, *28*, 1799–1809.
- (5) Unz, R. F.; Farrah, S. R. *Appl. Environ. Microbiol.* **1976**, *31*, 623–626.
- (6) Leppard, G. G. In *Environmental Particles*; Buffle, J., van Leeuwen, H. P., Eds.; Lewis Publishers: Boca Raton, 1992; Vol. 1, pp 231–289.
- (7) Massalski, A.; Leppard, G. G. *J. Fish. Res. Board Can.* **1979**, *36*, 906–921.
- (8) Leppard, G. G.; Massalski, A.; Lean, D. R. S. *Protoplasma* **1977**, *92*, 289–309.
- (9) Massalski, A.; Leppard, G. G. *J. Fish. Res. Board Can.* **1979**, *36*, 922–938.
- (10) Leppard, G. G. *Water Pollut. Res. J. Can.* **1985**, *20*(2), 100–110.
- (11) Decho, A. W. *Oceanogr. Mar. Biol. Annu. Rev.* **1990**, *28*, 73–153.
- (12) Droppo, I. G.; Stone, M. *Hydrol. Proc.* **1994**, *8*, 101–111.
- (13) Stone, M.; Droppo, I. G. *Hydrol. Proc.* **1994**, *8*, 113–124.
- (14) Droppo, I. G.; Ongley, E. D. *Water Res.* **1992**, *26*, 65–72.
- (15) Luft, J. H. *Anat. Res.* **1971**, *171*, 347–368.
- (16) Hanke, D. E.; Northcote, D. H. *Biopolymers* **1975**, *14*, 1–17.
- (17) Burnison, B. K.; Leppard, G. G. *Can. J. Fish. Aquat. Sci.* **1983**, *40*, 373–381.
- (18) Hayat, M. A. *Fixation for Electron Microscopy*; Academic Press: New York, 1981.
- (19) Spurr, A. R. *J. Ultrastruct. Res.* **1969**, *26*, 31–43.
- (20) Frosch, D.; Westphal, C. *Electron Microsc. Rev.* **1989**, *2*, 231–255.
- (21) Perret, D.; Leppard, G. G.; Muller, M.; Belzile, N.; De Vitre, R.; Buffle, J. *Water Res.* **1991**, *25*, 1333–1343.
- (22) Mavrocordatos, D.; Lienemann, C.-P.; Perret, D. *Microchim. Acta* **1994**, *117*, 39–47.
- (23) Leppard, G. G. *Analyst* **1992**, *117*, 595–603.
- (24) Wagner, M.; Abmus, B.; Hartmann, A.; Hutzler, P.; Amann, R. J. *Microsc.* **1994**, *176*, 181–187.
- (25) Li, D. H.; Ganczarczyk, J. J. *Environ. Sci. Technol.* **1989**, *23*, 1385–1389.
- (26) Ganczarczyk, J. J.; Zahid, W. M.; Li, D. H. *Water Res.* **1992**, *26*, 1695–1699.
- (27) Caldwell, D. E.; Korber, D. R.; Lawrence, J. R. *Adv. Microb. Ecol.* **1992**, *12*, 1–67.
- (28) Pawley, J. B. *Handbook of Biological Confocal Microscopy*, rev. ed.; Plenum Press: New York, 1990.
- (29) Horowitz, A. J. *A Primer on Sediment-Trace Element Chemistry*; Lewis Publishers Inc.: Chelsea, MI, 1991.
- (30) Costerton, J. W.; Cheng, K.-J.; Geesey, G. G.; Ladd, T.; Nickel, J. C.; Dasgupta, M.; Marrie, T. J. *Annu. Rev. Microbiol.* **1987**, *41*, 435–464.
- (31) Liss, S. N.; Allen, D. G. *J. Pulp Paper Sci.* **1992**, *18*, J216–221.
- (32) Fulthorpe, R. R.; Liss, S. N.; Allen, D. G. *Can. J. Microbiol.* **1993**, *39*, 13–24.
- (33) Leppard, G. G.; Burnison, B. K.; Buffle, J. *Anal. Chim. Acta* **1990**, *232*, 107–121.
- (34) Karl, D. M. *EOS* **1982**, *63*, 138–140.
- (35) Geesey, G. G.; Richardson, W. T.; Yeomans, H. G.; Irvin, R. T.; Costerton, J. W. *Can. J. Microbiol.* **1977**, *23*, 1733–1736.
- (36) Leppard, G. G. *Water Res.* **1986**, *20*, 697–702.
- (37) Paerl, H. W. *Microb. Ecol.* **1975**, *2*, 73–83.
- (38) Ganczarczyk, J. J. *Activated Sludge Process*; Marcel Dekker: New York, 1983.
- (39) Ellwood, D. C.; Tempest, D. W. *Adv. Microb. Physiol.* **1972**, *7*, 43–47.

Received for review June 19, 1995. Revised manuscript received September 20, 1995. Accepted September 22, 1995.*

ES950426R

* Abstract published in *Advance ACS Abstracts*, December 1, 1995.